Critical Reviews™ in Biomedical Engineering, 36(5–6), 441–471 (2008)

Hybrid Superporous Scaffolds: An Application for Cornea Tissue Engineering

Arpita Kadakia,[1] Vandana Keskar,[2] Igor Titushkin,[1] Ali Djalilian,[3] Richard A. Gemeinhart,[1,2] & Michael Cho[1*]

[1]Department of Bioengineering, University of Illinois, Chicago, IL; [2]Department of Biopharmacuetical Sciences, University of Illinois, Chicago, IL; [3]Department of Ophthalmology and Visual Science, University of Illinois, Chicago, IL

*Address all correspondence to Michael Cho, Department of Bioengineering (M/C 063), University of Illinois, Chicago, 851 S. Morgan St., Chicago, IL 60607; Tel. 312–413–9424; Fax: 312–996–5921; mcho@uic.edu.

ABSTRACT: Engineering a cell-based keratoprosthesis often requires a struggle between two essential parameters: natural 3-D biological adhesion and mechanical strength. A novel hybrid scaffold of natural and synthetic materials was engineered to achieve both cell adhesion and implantable strength. This scaffold was characterized in terms of cell adhesion, cell migration, swelling, and strength. While the study was focused on engineering a biointegrable prosthetic skirt, a clear central core with an appropriate refractive index and light transmission was also incorporated into the design for potential functionality. The hybrid scaffold was tested in rat corneas. This uniquely designed scaffold was well tolerated and encouraged host cell migration into the implant. The hybrid superporous design also enhanced cell adhesion and retention in a superporous scaffold without altering the bulk mechanical properties of the hydrogel.

KEY WORDS: keratoprosthesis, artificial cornea, 3-D hybrid scaffold, superporous hydrogel, collagen, polyethylene glycol diacrylate

ABBREVIATIONS

PMMA	polymethyl methacrylate
PHEMA	poly(2-hydroxyethyl methacrylate)
ECM	extracellular matrix
PEG	polyethylene glycol
PAA	polyacrylamide
SPH	superporous hydrogels
PEGDA	polyethylene glycol diacrylate
hMSC	human mesenchymal stem cells
SIPN	semi-interpenetrating network
TRITC	tetramethylrhodamine isothiocyanate
DAPI	4,6-diamidino-2-phenylindole
AFM	atomic force microscope
SHG	second harmonic generation

0278-940X/08 $35.00

I. INTRODUCTION

I.A. Background and Significance

The cornea is an avascular and optically transparent tissue that refracts and filters light rays before they enter the eye. A clear cornea is essential for clear vision. The cornea may become opacified following injuries, degenerations, or infections. The Vision Share Consortium estimates that corneal blindness affects more than 10 million patients worldwide.[1] The gold standard treatment is surgical replacement of the cornea using freshly donated human cadaver corneas. Corneal transplantation is currently the most common form of organ transplant performed in the United States.[2] About 40,000 corneal transplants are performed each year in the United States,[3] with a 2-year success rate as high as 90% for uncomplicated first grafts performed in nonvascularized, "low-risk" patients.[4,5] Successful transplantation depends on the quality and availability of a donor cornea as well as the patient's underlying condition. However, the success in low-risk corneal transplantation contrasts sharply with the results of corneal grafts placed in so-called "high-risk" patients, in whom rejection rates can increase up to 50%–70%, even with maximal local and systemic immune suppression.[6,7] Currently, up to 10% of patients are considered high risk and have a significant chance of rejection after transplantation.[6,7] Immune-mediated rejection is the leading cause of corneal transplant failure.[8,9] The risk factors for immunologic rejection include previous graft rejection, corneal vascularization, and young age. These high-risk patients typically undergo repeated surgeries, resulting in excessive pain, cost, and use of limited resources. A major advantage of an artificial cornea is the absence of immune rejection.

While the need for artificial corneas in the United States is primarily driven by the high-risk population that cannot tolerate donor grafts, the global need is driven by both the high-risk population *and* the severe shortage of donor corneas.[10] Additionally, demands for donor corneas are projected to increase in the near future because LASIK-treated corneas are unacceptable as donors.[1] The above factors suggest that there is a demand for an alternative therapy to donor cornea transplantation. Tissue-engineered corneal implants can provide an alternative for patients who cannot receive or do not respond well to donor corneas.

I.B. Keratoprostheses

In 1771, Pellier de Quengsy is credited with the first attempt to implant a foreign material, glass, in the cornea.[11] In the 1800s, other materials such as quartz, tantalum, vitallium, and celluloid were used unsuccessfully in attempts to create an artificial cornea.[11,12] With the advent of donor cornea transplantation, the idea of an artificial cornea was abandoned as more attention was given to refining donor keratoplasty techniques. It was not until World War II, when it was observed that polymethyl methacrylate (PMMA) was biocompatible in the human eye, that the idea of an artificial cornea resurfaced. Unfortunately, biocompatibility was not sufficiently acceptable for a good artificial cornea, because keratoprostheses made from PMMA still had the problem of extrusion. Many, including Girard and Cardona, have tested different designs and materials, however, long-term retention remains a major problem.[11,12]

There are three general types of keratoprostheses: nonpenetrating, penetrating, and perforating. In a nonpenetrating keratoprosthesis, a two-stage procedure is used in which the implant is placed intrastromally, the periphery is allowed to integrate with the host stroma, and then the posterior cornea is removed. This technique was not initially successful because the implant prevented diffusion of aqueous humor to tissue anterior to the implant, and without nutrients this tissue would necrose. However, with changes in the type of material used to increase diffusion, this technique is becoming popular again because it avoids the need for suturing.

A penetrating keratoprosthesis is for corneas that have partial thickness opacification (the cornea is not uniform throughout). In certain disease states, just the anterior or posterior portion may be damaged. In this technique, an optically clear cylinder is inserted in place of the opacified portion and an intralamellar ring is used to anchor the device. As was the case for nonpenetrating keratoprostheses, necrosis anterior to the device is the major problem with this technique.

A perforating keratoprosthesis uses a through and through hole. A clear core is placed in the center through all layers of the cornea and, similar to the penetrating type, an intralamellar ring holds the device in place. While clarity is improved, there is a higher rate of extrusion. This is again due to tissue necrosis, in this case anterior to the ring, and retroprosthetic membrane formation.

Many variations to each type of keratoprosthesis have been developed, but the underlying pitfall with all of them seems to be a lack of nutrient diffusion resulting in anterior tissue death and ultimate extrusion of the device. Currently, there are two FDA-approved keratoprostheses available for transplantation, the Boston Keratoprosthesis (KPro) and AlphaCor.[13] The most common challenge and limitation of current artificial corneas is their lack of incorporation into host tissue, which can lead to infection, tissue necrosis (melting), or spontaneous rejection (extrusion).[14]

1. KPro

The KPro pioneered the modern core-and-skirt design in which a bio-integrable skirt surrounds an optically clear core.[15] It is one of the most commonly used keratoprostheses in the United States.[16] The design of the KPro consists of three parts: a PMMA core, a donor cornea graft, and a PMMA or titanium back plate. The core screws into the back plate, sandwiching the donor cornea in between. Many modifications have been made to this design since 1974, when the device was first implanted in patients, because it was observed that many patients seemed to develop glaucoma post-implantation. Because corneal elasticity contributes to damping of intraocular pressure,[17] there is some speculation that the rigid materials used in this prosthesis may induce elevating intraocular pressures.[1] However, some clinicians believe that many of these patients may have had predisposing conditions that caused them to develop glaucoma.[18] Despite the origin, high pressure can cause disassociation of the core and skirt. Therefore, a titanium ring was introduced to the device, which snaps at the posterior aspect and secures the core and skirt together to prevent potentially rising intraocular pressure from unscrewing the core.

Another adjustment was made after researchers noticed that the donor cornea suffered from a lack of nutrients resulting in tissue necrosis. Realizing that the cornea receives most of its nutrition from the aqueous humor, eight small holes were added to the back plate to allow for some diffusion between the humor and the donor cornea. This adjustment resulted in a significant reduction in tissue melt around the core, from 51% to 10%.[16]

2. AlphaCor

AlphaCor has a similar core-and-skirt design, but contains a soft polymer to avoid the complications associated with the rigidity of the KPro. This polymer is poly(2-hydroxyethyl methacrylate) (PHEMA), which has been used extensively in ocular devices, including contact lenses, intraocular lenses, and intracorneal inlays. The distinguishing feature of AlphaCor is the microporous polymer skirt. It is created by phase separation of PHEMA and water during polymerization, and serves to provide more natural diffusion of nutrients and cell migration than much larger holes.[14]

Although fibroblasts were shown to migrate in and secrete extracellular matrix (ECM), long-term human studies revealed numerous complications such as reduced biointegration.[19] There was also unexplained calcification of the skirt over time. The core is made of the same material as the skirt, but without the phase separation so that it is optically clear. The core is polymerized after the skirt, allowing interpenetration of the core periphery into the skirt, creating a secure bond between the core and skirt. As a soft hydrogel, however, PHEMA has a tendency to undergo discoloration due to environmental factors or medications.

Both the KPro and the AlphaCor have high retention rates: AlphaCor is reported to have a 92% retention after 6 months[20] and KPro 95% after 8.5 months.[21] However, neither is widely accepted due to a lack of stable host integration that eventually results in melting, extrusion, and rejection.[14] Also, wound healing in these devices is prolonged, and stromal cells seem to remain in an activated fibroblastic state.[16] One explanation for this is that a lack of epithelialization over the device continually stimulates underlying fibroblasts. In addition, the deficiency in epithelial cells over the anterior surface renders the eye unprotected and susceptible to infections.[22] For these reasons, artificial corneas are rarely used in clinical practice and are reserved for patients who have failed all standard therapies.

To overcome the previously mentioned limitations, many investigators have tried other polymers and techniques. Myung et al.[22] developed a polyethylene glycol (PEG)/polyacrylamide (PAA)-based copolymer in which the skirt is photopatterned with pores. While the pores can provide a physical pathway for cellular migration from host to implant, they do not provide biological cues for cells to adhere. They do, however, attach type 1 collagen to the anterior surface for epithelial overgrowth. Realizing the need for biological adhesion in the stroma, Liu et al. created a collagen-based artificial cornea[23] that exhibits good stromal cell in-growth. Grafting of the laminin attaching peptide YIGSR also showed nerve cell attachment. A cross-linker is required to increase the mechanical strength of collagen and prevent in vivo degradation by active matrix metalloproteinases. Liu et al. recommend very high collagen concentrations (9% w/w versus traditionally used 1% w/w). Cross-linking and high concentrations pose a challenge for 3-D cell pre-seeding, a major facet of this cell-based device. The investigators also grafted alginate to the posterior aspect by plasma treatment to reduce endothelialization. Sheardown and Duan introduced dendrimer cross-linked collagen as having higher transparency.[24] Tissue melting and skirt exposure was observed in all cases.[14] Fenglan et al. developed a combined biosynthetic device consisting of nano-hydroxyapatite and poly(vinyl alcohol).[25] Porosity was created by salt leaching to prevent pre-seeding of cells. The mechanical properties of this scaffold were favorable: both elastic and strong to hold sutures. Garty et al. have created a hybrid structure of porous PHEMA and collagen.[26] Their pores were created by templating around microspheres with collagen grafted to the pore wall; they have shown cell adhesion to the collagen, and by narrowing their pore size they were able to achieve 3-D like cell behavior.[26] Alaminos et al.[27] created a full-thickness, cell-based artificial cornea by culturing all three cell types using a fibrin-agarose scaffold. Cells were cultured sequentially using a trans-well culture insert starting with the endothelial layer. After 2 weeks, a corneal equivalent was ready for use. Fibrin gels, in contrast to collagen, do not contract when cells are embedded within. Therefore, this gel is more likely to maintain transparency. In vivo results are not yet published. The developments of the KPro and AlphaCor prostheses, as well as many others, have made significant strides toward artificial cornea design. The hybrid scaffold presented here builds upon these models to engineer a truly biointegrable device with natural 3-D cell-binding sites, stability, clarity, and biocompatibility.

I.C. Cornea Architecture

The cornea is the anterior-most portion of the globe, functioning as a clear front window that also protects the eye from mechanical and chemical damage. It is an avascular structure (to maintain clarity) that meets its oxygen and nutrient requirements from the tear film and aqueous humor, respectively. The human cornea has a diameter of 11 mm, with a thickness of about 0.5 mm centrally and 1 mm peripherally. Being the first structure to interact with incoming light, the cornea is the major refractive component of the eye. About 80% of refraction is accomplished at the air-cornea interface; the remaining 20% is refracted by the lens. Within the cornea, refraction occurs at three interfaces: air-tear, tear-cornea, and cornea-aqueous humor. The refractive indices of tears and humor are both 1.336. The human cornea has a refractive index of 1.376. Therefore, it is necessary to maintain this index in our engineered model to provide appropriate refraction for the patient.[12] Corneal tissue engineering is particularly challenging because it requires the incorporation of several cell types in distinct layers while maintaining clarity and a proper refractive index. Five layers comprise the human cornea: the epithelium, Bowman's layer, stroma, Descemet's membrane, and endothelium.

1. Epithelium

The epithelium is the outermost layer of the cornea. It is composed of squamous epithelial cells and occupies 10% of the tissue's thickness. The epithelium itself is comprised of four cell layers: a superficial layer of flattened cells with villi to adhere to the tear film, an intermediate layer of polyhedral cells, a basal germinal cell layer that functions to regenerate upper cell layers (similar to skin), and a bottom layer attached to Bowman's membrane. The main functions of the epithelium are to block foreign materials from entering the eye and to absorb oxygen from the tear film. An intact epithelium maintains a barrier against infection and signals underlying fibroblasts to remain quiescent. Epithelial cells are exposed to a polarized environment: the tear-cornea interface. Engineering this layer would best be accomplished by exposing cells to a similar environment with 2-D culture conditions.

2. Bowman's Layer

Bowman's layer is an acellular sheet of collagen separating the epithelium from the stroma. Injury to this area can result in scarring and stromal cell migration to the surface, both of which can contribute to vision loss. The Bowman's layer is attached on the sides at the limbus, assuming a dome-like shape responsible for the curvature of the cornea. Engineering this layer should not be overlooked. It is important to separate the epithelium from the underyling stroma, because cell growth in the wrong layer can lead to opacities. The curvature of the engineered cornea should be provided at this layer.

3. Stroma

The stroma, located beneath Bowman's layer, comprises about 90% of the cornea's thickness. It is composed of water, collagen, elastin, proteoglycans, and keratocytes. Major proteoglycans present are dermatan sulfate in the anterior and keratan sulfate in the posterior. Dermatan sulfate helps to retain water and keratan sulfate helps to absorb water. Keratocytes are quiescent cells in vivo that synthesize collagen and proteoglycans. The term "quiescent" here does not denote a state of inactivity, but rather a lack of proliferation. In vitro culture in the presence of serum activates keratocytes, causing a rapid proliferation of corneal fibroblasts.[28] Keratocytes have a large nucleus, a prominent Golgi complex, and cytoplasmic processes that extend in all directions. Keratocytes synthesize type 1 collagen. Collagen comprises about 70%

of stroma's dry weight. A difficult to replicate, unique arrangement of collagen in the cornea provides both strength and transparency. Corneal keratocytes are capable of producing collagen fibers and arranging them in this lattice structure. From an engineering perspective, creating an environment in which cells can function to make their own ECM, thereby mimicking the arrangement and size of natural stroma, is likely to produce a transparent structure. As opposed to epithelium, cells in this layer are most natural in a 3-D ECM. The major focus of the present study was to create such an environment for corneal fibroblasts.

4. Descemet's Membrane

Below the stroma lies Descemet's membrane, another acellular layer that separates the stroma from the endothelium. Descemet's membrane is the basal lamina produced by endothelial cells.

5. Endothelium

The endothelium is the innermost layer of the cornea, and serves as a pump to regulate the hydration level of the cornea via sodium-potassium exchangers It is a single cell layer thick, and each cell forms tight appositions to neighboring cells to prevent any leakage of aqueous humor into the stroma. Thus, engineering of the posterior aspect of a keratoprosthesis should be permeable to nutrients yet prevent significant aqueous humor leakage.

I.D. 3-D Superporous Scaffolds

Cells respond differently to extracellular cues presented in a 3-D versus a 2-D context. Cell adhesion is markedly altered in 2-D due to the artificial polarity created by the air-substrate interface (except epithelial cells). A 3-D extracellular environment is a key component contributing to the success of a tissue-engineering scaffold. Despite the evidence encouraging 3-D tissue-engineering scaffolds, however, they are largely limited by diffusion capabilities. Long-term cell-based devices that are 3-D suffer from the "M&M" effect: cells in the center tend to die from a lack of nutrition because diffusion of nutrients into the depths of the scaffold is not adequate, and this results in these cells resembling an M&M candy: a soft core and hard outer shell. Therefore, a porous system is necessary to facilitate nutrient and waste exchange throughout the construct.[29] Pores are also advantageous post-implantation, when they can serve as conduits for host cell integration. The surrounding

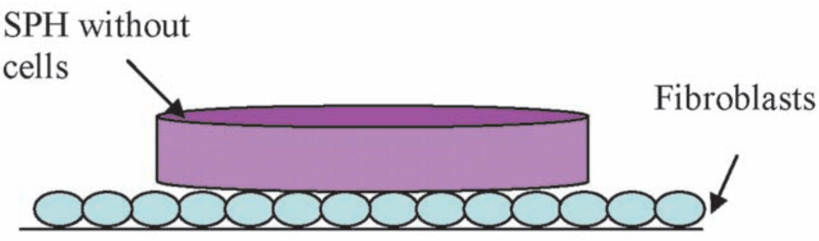

FIGURE 1. An in vitro model of host cell integration was created by placing an acellular SPH over a monolayer of cells. Live/dead dye was utilized to visualize the extent of cell integration into SPH scaffolds with and without collagen.[31]

tissue, including blood vessels and neurons, can migrate into the scaffold via the interconnected pore network, further cementing the construct within the tissue.

Many methods have been employed to engineer 3-D porous scaffolds, including salt leaching, freeze-drying, and layer-by-layer lithography using heat, adhesives, light, or molds. While these methods have many advantages, major drawbacks include difficulty in achieving interconnected pores, toxic by-products, difficulty incorporating cells, and long processing times.[30] We consider superporous hydrogels (SPH) as ideal 3-D porous tissue-engineering scaffolds because the fabrication method overcomes many of these challenges. SPHs are easily created by a foaming reaction optimized for simultaneous polymerization. This results in a 3-D, interconnected pore network with macroscale pores. "Superporous" implies that the scaffold swells rapidly in solution (<1 min). This technology can be utilized to "suck up" soluble materials such as cells and proteins within the SPH, thus creating a 3-D hybrid superporous scaffold (Fig. 1) (V.A.K. et al., unpublished data, 2009).

II. MATERIALS

II.A. Collagen

Collagen is a natural component of human extracellular matrix. In vivo, collagen provides tensile strength as well as binding sites for many cell types, and is nontoxic, biodegradable, and inexpensive. In our hybrid scaffold, type 1 collagen functions to encourage stromal cell adhesion, host integration, and surface epithelialization. Collagen is solubilized in acetic acid to its non-fibrillar form and undergoes fibrillogenesis to form a gel network (thermogelation). In vivo, this is a structured process in which microfibrils line up end to end, laterally producing a characteristic 65 nm banding pattern.[31] However, in vitro, fibrils join together in a haphazard, random fashion. Therefore, this network is significantly weaker than in vivo collagen fibers. It may also relate to the lack of transparency observed in in vitro collagen gels. To increase the mechanical stability of collagen, many investigators have attempted chemical cross-linking, dehydration, or compression. However, such methods are often toxic to cells and prevent 3-D encapsulation of cells within the matrix. To overcome this issue, we are attempting to reinforce collagen gels with polyethylene glycol diacrylate (PEGDA), thus retaining the significant positive cell-influencing aspects of collagen as a biomaterial while also gaining additional properties of PEGDA.[32]

II.B. PEGDA

Synthetic polymers such as PEGDA are attractive scaffold materials because their chemical and physical properties are controllable and reproducible. Altering molecular weights, block structures, degradable linkages, and cross-linking modes can influence gel formation kinetics, cross-linking density, and mechanical and degradation properties.[32] In addition, synthetic materials are free of antigenic responses. Hydrogels are water-swollen, cross-linked polymers that have material properties similar to the ECM of many tissue types.[33] ECM is composed of two main classes of molecules: polysaccharide chains, or GAGs, and fibrous proteins such as collagen. GAGs form a highly hydrated gel with mechanical properties comparable to synthetic hydrogels. Both hydrogels and GAGs are hydrophilic and occupy a large volume. Therefore, they can function as shock absorbers to withstand compressive forces.

1. Hydrogels as Biomaterials and a Model System

Hydrogels are water-swollen polymeric networks containing cross-links that may be chemical bonds, crystallites, physical entanglements, or weak associations such as hydrogen bonds. Hydrogels have been developed as "blood-compatible" materials and as implantable materials in many applications.[34–36] Many monomers can be used to form hydrogels for medical uses, but PEG-based hydrogels have emerged as excellent materials due to their favorable, nontoxic properties.[36,37] The main reason for the utilization of hydrogels in biologic environments is that they are very similar to natural tissue in regard to hydration and mechanical properties.[38] Although the properties that make hydrogels excellent candidates for this application (and many other biomedical applications) are numerous, several are of vital importance in this application. First, hydrogels have a defined mesh size that determines the size of molecules that can move through the network, and this can be determined from the swelling of hydrogels in various fluids.[34] The mesh size is the "free space" that is available for diffusion of molecules in the hydrogel. Secondly, hydrogels do not readily adsorb or denature proteins due to the hydrated nature of the polymer network. In fact, PEG hydrogels have been used to stabilize proteins,[39] and PEG polymer chains are used clinically for this purpose.[40] This is predominantly due to greater mobility of the polymer chains near the surface of the hydrogels, which act like a "polymer brush."[41] Due to the lack of protein adsorption, cells do not readily attach to hydrogel surfaces[42] unless specific protein-binding sequences are incorporated.[43,44] A recent review cited hydrogels as having minimal injury responses similar to those seen without a hydrogel, while hydrophobic devices showed extensive foreign-body reaction.[45] Because hydrogels have excellent biocompatibility and the ability to allow entry of proteins without denaturation, they are excellent materials for examining cell-solid matrix interactions and material-host interactions.

2. PEGDA-based Superporous Hydrogel

We have adapted the original polyacrylamide-based SPH to a PEGDA-based SPH.[46] PEGDA is an attractive implantable material because its physical properties can be tunable to match the desired tissue type. In addition, PEGDA is optically clear, rendering it ideal for microscopy studies using in vitro and in vivo applications in which clarity is essential. This quality has made PEGDA the subject of many surface modification studies. For example, it has been incorporated with matrix metalloproteinases, oligopeptide sequences, and integrin-binding peptides such as RGD. However the isolated insertion of a few biological signals cannot compete with the entirety of signals provided by natural ECM proteins in 3-D. In this paper, we have described a method to incorporate natural materials within a PEGDA-SPH network. This method can be extended to incorporate additional molecules as necessary for individual cell types and tissue applications (V.A.K. et al., unpublished data, 2009).

II.C. Cell Types Utilized

Two cell types, stem cells and committed cells (fibroblasts), were tested utilizing this method. Human mesenchymal stem cells (MSC) were obtained from The Center for Gene Therapy at Tulane University. MSC were maintained in GIBCO α-minimal essential medium (with L-glutamine, without ribonucleosides, without deoxyribonucleosides; Invitrogen, Carlsbad, CA) containing 15% fetal bovine serum, 1% L-glutamine, and 1% antibiotics. MSC are ideal for many types of tissue engineering because they can often be obtained from the patient's own bone marrow, therefore reducing issues of immune rejection and avoiding the use of controversial embryonic stem cells.

If the patient's own cells are healthy, stem cell differentiation may not be necessary. Two fibroblast cell lines were purchased: the HT-1080 fibrosarcoma cell line and the CCL-60 corneal fibroblast cell line (ATCC, Manassas, VA). Fibroblasts were bathed in Dulbecco's modified eagle's medium supplemented with 10% fetal bovine serum and 1% antibiotics/antimycotics. All cells used in these experiments were between passages 3 and 6. The method presented here can be extended to other cell types. Cells can be either loaded into the scaffold prior to implantation or can be encouraged to migrate into the scaffold post-implantation. This study evaluated both scenarios.

III. METHODOLOGY

III.A. Hybrid Scaffold

We created a hybrid scaffold in which the PEGDA polymer was utilized as a framework and the collagen chains as anchors to encourage cell adhesion. PEGDA was cross-linked for structural support. Collagen was not cross-linked because this risks altering the structure of the chain and interfering with natural 3-D cell binding. Initially a semi-interpenetrating network (SIPN) was attempted by mixing the two polymer solutions with cells prior to gelation.

III.B. Superporous Hydrogel Fabrication

Based on results from the SIPN method, it seemed necessary to separate gelation of collagen and PEGDA both spatially and temporally to create a hybrid with true 3-D cell adhesion. This was accomplished using superporous PEGDA. A 20% (w/v) PEGDA solution (500 uL) was combined with the following reagents: 60 uL of 10% pluronic PF 127, 30 uL of 20% Temed, 20 uL of acrylic acid, and 23 uL of ammonium persulfate. The final volume was adjusted to 1 mL via addition of deionized water. The solution was heated for 2 min at 37°C. Finally, 200 mg of sodium bicarbonate was mixed in the solution, which created a foaming reaction resulting in a porous structure. The amount of sodium bicarbonate was varied from 100 to 300 mg to create differences in pore architecture. SPHs were rinsed in water to remove unreacted sodium bicarbonate crystals. To prevent pore collapse, the scaffolds were dehydrated in ethanol overnight, and then further dehydrated in a food dehydrator for 45 min. Cut sections were sterilized under UV light for 20 min (V.A.K. et al., unpublished data, 2009).[46]

III.C. Collagen Gel

Rat tail collagen type I (BD Biosciences, San Jose, CA) was mixed with 0.1 N NaOH, 10X Hank's balanced salt solution, and 0.1 N acetic acid at a volume ratio of 3:2:1:1 to create a neutral pH collagen solution at a concentration of 1 mg/mL.[47] If cell seeding was desired, cells were suspended in the collagen solution at a concentration of 1 million cells per milliliter to encapsulate them in a 3-D network. Soaking a dehydrated SPH in this solution allowed uptake of cells and collagen within the pores. Collagen gelation was initiated by warming to 37°C for 30 min. If pre-seeding with cells was not desired, the SPH was soaked in the collagen solution without cells, and, again, gelation occurred by warming to 37°C for 30 min.

III.D. Cell Adhesion

Effects of the environment exerted on cells often determine cell morphology. For example, the lack of integrin-binding sites within PEGDA forces cells to assume a round morphology, whereas collagen allows cells to form focal adhesions, sprawling and spreading out as necessary. SPH constructs with and without collagen were employed as 3-D fibroblast scaffolds. Cells were loaded in the pre-seeded method as described above and incubated for 24 and 48 h. A Chemicon focal adhesion kit (Millipore, Billerica, MA) was used to visualize cell adhesion and retention. tetramethylrhodamine isothiocyanate (TRITC)-phalloidin stained microfilaments red and 4,6-diamidino-2-phenylindole (DAPI) stained nuclei blue. A confocal microscope (Bio-Rad, Hercules, CA) was used to image each of these structures.

Phalloidin is the most common dye used to image actin filaments. The cytoskeleton regulates many cell functions, including cell movement, cell-ECM binding, and structural support. To do all of this, the actin cytoskeleton must be quite organized. It is a dynamic structure that changes in response to extracellular cues. Stress fibers are bundles of actin filaments that develop in cells adhered to the external environment. They terminate at the cell membrane in focal adhesions that consist of proteins that connect the internal cytoskeleton to the external ECM. Stress fibers correlate to a cell's ability to grip the ECM for the cell to adhere. They can also transmit mechanical signals to the ECM. By tugging on collagen fibers they can reorganize the fibers around the cells. Therefore, visualization of this structure using TRITC-phalloidin provides insights into and confirmation of cell adhesion within the scaffold. DAPI is a blue fluorescent stain that binds strongly to DNA, confirming the presence of cells.

III.E. Host Cell Integration

In cases where pre-seeding with cells was not desirable, we tested whether our hybrid scaffold was preferred for cell migration. Acellular SPH scaffolds with and without collagen were placed atop a monolayer of cells (Fig. 1). Cell migration into the scaffold was monitored over 3 weeks. Cells were stained with live/dead viability and visualized with the confocal microscope. This study aimed to model which scaffold would be preferred for in vivo host cell migration. Results from the cell migration experiments are expected to provide guidance for animal model studies and eventually clinical trials regarding the requirement of pre-seeding cells to promote the implant-host integration.

III.F. Swelling Ratio

Rapid swelling to large volumes is an important feature for this application. The SPH fabrication method created interconnected macrosized pores, and swelling occurred in less than 1 min. Since collagen begins to gel quickly after pH neutralization, immediate upload into the SPH is necessary to facilitate uniform distribution throughout the SPH. A swelling ratio, Q, was determined by comparing the mass of the swollen SPH to the mass of the dehydrated SPH. Dehydrated structures of varying pore sizes were soaked in water for at least 20 min. All SPHs were centrifuged at 1000 rpm for 3 min to remove air bubbles. SPHs were strained with a sieve to remove excess water and weighed. This mass represents the water accumulated in the pores as well as in the hydrogel structure itself. Next, the SPHs were gently squeezed and blotted with a Kimwipe (Kimberly-Clark, Dallas, TX) to remove water in the pores but maintain water in the hydrogel structure. By dividing the swollen weight by the initial weight, two swelling ratios, $Q_{\text{Total Water}}$ & $Q_{\text{Hydrogel Water}}$, were obtained (V.A.K. et al., unpublished data, 2009).

$$Q_{\text{Total Water}} = \text{Weight}_{\text{Total Water}}/\text{Weight}_{\text{Dehydrated}}$$

$$Q_{\text{Hydrogel Water}} = \text{Weight}_{\text{Hydrogel Water}}/\text{Weight}_{\text{Dehydrated}}$$

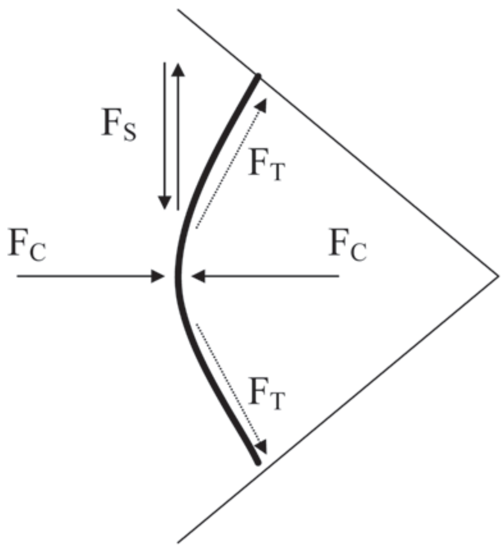

FIGURE 2. Physiological forces that will be experienced by the implant. In this schematic, F_c is compressive forces from the atmosphere and intraocular pressure, F_s is shear forces from blinking; F_T is depicted with dotted lines to indicate the tensile force that will arise later from the host tissue once it begins to bond with the implant. Any successful implants would have to be engineered to demonstrate mechanical compatibility.

III.G. Mechanical Testing

Based on the stresses that the artificial cornea would undergo in vivo, multiple methods of mechanical testing were employed to determine the strength of the scaffold. The schematic in Figure 2 predicts the combination of forces acting upon an artificial cornea.[48] Prostheses are subjected to compressive forces (F_C) by the aqueous humor and atmospheric pressure, and also experience shear forces (F_S) due to blinking. If they were to be sutured, there would be immediate tensile forces (F_T). However, since our surgical procedure does not include suturing, this is negligible initially. After time has elapsed and host integration takes place, we can assume that there would be some tensile forces created by the natural tissue. Compressive and tensile moduli were tested.

1. Compressive Testing

The compressive modulus of the SPH scaffolds was determined by compressive testing. Water-swollen SPHs were sandwiched in between two pieces of glass lined with Velcro (to prevent slippage) and compared with collagen-swollen SPHs and SPHs made with different amounts of sodium bicarbonate. The amount of strain that each SPH withstood was recorded. A stress versus strain curve was plotted to determine an estimate of compressive modulus.

2. Tensile Testing

An atomic force microscope (AFM; Novascan, Ames, IA) was used to measure the mechanical properties using an indentation technique. The AFM was used to determine the Young's modulus of the hybrid scaffold. This method is preferred to traditional tensile testing, which can damage the sample at the grip points. This is especially useful when working with soft tissues such as hydrogels. Micro-indentation force-curves can be obtained using the AFM with a 10 μm glass bead attached to the cantilever. A bead rather than a regular sharp AFM tip decreases data variation due to inhomogeneity. The Young's modulus is calculated using the Hertz model:

$$F_{sphere} = \frac{4}{3} \cdot \frac{E}{(1-\nu^2)} \cdot \delta^{3/2} \cdot \sqrt{R} = k \cdot d$$

where F is the indenting force, R is the attached bead radius, δ is the indentation, assuming that δ<< R, E is Young's modulus, ν is Poisson ratio (0.5 for incompressible sample), k is the cantilever's spring constant, and d is the cantilever's deflection. This model assumes a homogeneous, isotropic, semi-infinite elastic material. Furthermore, the surface should be flat, a conical or spherical tip should be used, and the indenter material should be much stiffer than the sample. A full description of the Hertz model and AFM-based mechanical measurements is provided elsewhere.[49]

III.H. Artificial Cornea Design

A prototype of the artificial cornea described above was created. A central hole was carved out of a dehydrated SPH disc, which was soaked in a fibroblast-collagen solution. As a control, SPHs were also soaked in cell solutions without collagen. Submersion in liquid causes rapid swelling of the SPH and uptake of collagen and cells within the pore network. Collagen fibers were then thermogelled. The result was a collagenous microenvironment dispersed noncovalently throughout a mechanically stable hydrogel. The central hole was filled with a nonporous, optically clear PEGDA macromer solution. The nonporous PEGDA solution diffused into the immediate periphery, spread along the bottom surface of the SPH, and deposited a thin layer of nonporous PEGDA on the anterior surface. The nonporous PEGDA was thermogelled into this irregular shape. Figure 3 is a schematic of prototype fabrication. A dehydrated

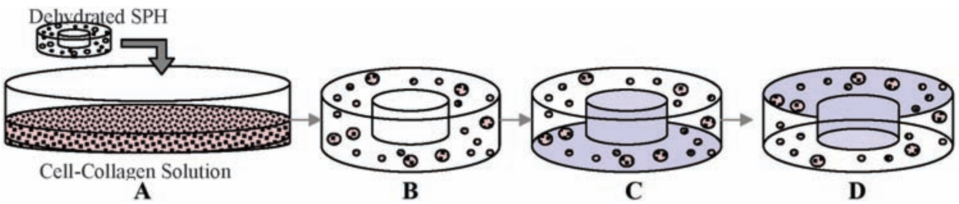

FIGURE 3. A dehydrated SPH is soaked in a collagen solution embedded with cells (A). This causes rapid swelling of the SPH and uptake of collagen and cells within the pore network (B). Collagen fibers are gelled by placing the construct in a 37°C incubator. The result is a collagenous microenvironment dispersed throughout a mechanically stable hydrogel. A prefabricated central hole is filled with nonporous, optically clear, photopolymerized PEGDA (C). The nonporous PEGDA diffuses into the immediate periphery of the SPH to create a seamless integration between the two components. A thin layer of nonporous PEGDA is polymerized over the entire anterior surface (D). This layer will be surface modified with collagen so epithelial cells can grow over the top.

SPH was immersed into the solution containing collagen and cells. As the SPH swelled, cells and collagen became entangled within the pores. After gelation, nonporous PEGDA filled the central hole and settled on the bottom surface. The bottom surface was flipped to generate a smooth anterior surface. Secure adhesion between the skirt and core was achieved by intense interdigitation between the nonporous and SPH PEGDA.

This proposed model mimics key aspects of natural cornea architecture. The anterior surface can be coated post-implantation with epithelial cells to encourage host epithelialization to regenerate the protective and nutrient-absorbing qualities of the epithelium. Below the epithelium, similar to Bowman's layer, a thin layer of nonporous PEGDA separates the epithelium from the underlying stroma. PEGDA discourages cell binding and keeps cell types localized. Within the stromal skirt, collagen and cells are surrounded by PEGDA, a hydrogel that is capable of retaining large amounts of water to maintain an appropriate shape and hydration level. The hybrid superporous skirt is designed to allow maximal host cell integration through the pores and attachment to cell adhesion sites. It may be difficult to replicate the intricate arrangement of collagen fibers to impart sufficient clarity, and thus the central core is kept free of collagen to maintain optical transparency. Future studies incorporating degradable linkages within the SPH could allow for long-term remodeling of the skirt ECM by stromal cells, resulting in eventual clarity and complete integration of the device.

III.I. Optical Data

Optical properties such as light transmission and refractive index of the central core were determined with a UV-Vis spectrophotometer and refractometer, respectively. The percentage of light transmittance was measured in reference to phosphate buffered saline at wavelengths ranging from 200 to 1000 nm.

III.J. In Vivo Testing

Sprague-Dawley rats were placed under general anesthesia with an intramuscular injection of ketamine (45 mg/kg) and xylazine (3–5 mg/kg) IM/SQ. A drop of proparacaine and a drop of ofloxacin were instilled in the right eye at the beginning of the procedure. Surgery was conducted under sterile conditions under an operating microscope. Only the SPH scaffold was implanted. One scaffold was the hybrid with collagen and the other was without collagen (control).

Ultimately this prosthesis will be implanted in a two-stage procedure using rabbits. In the first stage, the device will be implanted as a partial thickness replacement keeping the anterior cornea of the rabbit as a protective flap. In stage two, the portion of the anterior flap that covers the clear zone of the implant will be removed and the device will function as a full-thickness replacement. The rationale for this staged procedure is to maintain the integrity of the cornea while allowing time for integration to take place. After the flap is removed, the surface can be modified for epithelialization. The present study assessed biocompatibility at stage I.

1. Implantation of the Artificial Cornea (Stage I)

The rats were anesthetized and prepared as described above. A flap approximately 3 mm in diameter was created by slicing the cornea horizontally. The scaffold was sandwiched between the posterior and anterior regions of the cornea. The control rats received the same implants but without any collagen embedded in the skirt. The anterior flap was placed back on top of the implant and sutured to the peripheral cornea using interrupted dissolvable 10–0 vicryl sutures.

IV. RESULTS AND DISCUSSION

IV.A. Hybrid Scaffold

It was observed that simultaneous gelation of collagen and PEGDA as an SIPN resulted in a scaffold very similar to PEGDA alone. It had a

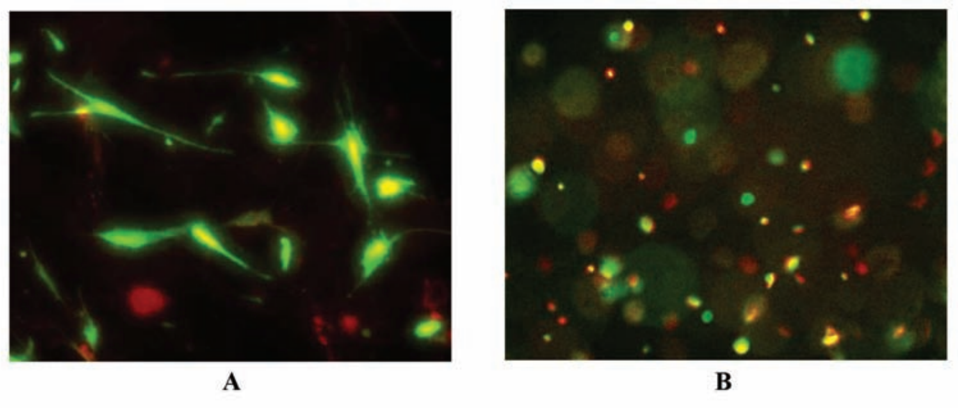

FIGURE 4. Human mesenchymal stem cells were seeded in 3-D gel. After 1 d, a live/dead viability dye was applied. Live green cells are seen spreading out due to cell-binding sites available in a collagen gel (A). Only few dead cells are seen as round and red. Despite the presence of collagen, cells are not able to spread in an SIPN PEGDA gel (B). While some live green cells are shown, there are also many dead red cells.

similar elastic modulus and could not achieve cell binding. Increasing the concentration of collagen still could not induce cell spreading. Figure 4 shows the difference in MSC cell morphology between a pure collagen gel and an SIPN of 10% PEGDA and 1mg/mL collagen, which shows that the SPIN scaffold is not adequate for cell viability and attachment.

The presence of PEGDA monomers during collagen gelation seemed to somehow alter the cell-binding capabilities of collagen. Imaging of collagen fibers with multiphoton microscope showed a lack of signal in second harmonic generation (SHG), a non-linear optical imaging technique that requires no flurophores. Collagen does not display an SHG signal when it has been denatured or altered. Therefore, separating the gelation of collagen and PEGDA both temporally and spatially was the next step in obtaining a true hybrid scaffold with these two materials. This was done by using superporous PEGDA intertwined with collagen gel, which resulted in natural cell binding to collagen. This separation isolates collagen to the pores, minimally interacting with PEGDA while maximally interacting with cells.

To confirm that collagen was in its natural fibrillar form and not affected by PEGDA, a multiphoton microscope was used to image these fibers. Two images were taken approximately 90 μm apart (Fig. 5). Collagen fibers are apparent and display an SHG signal. This

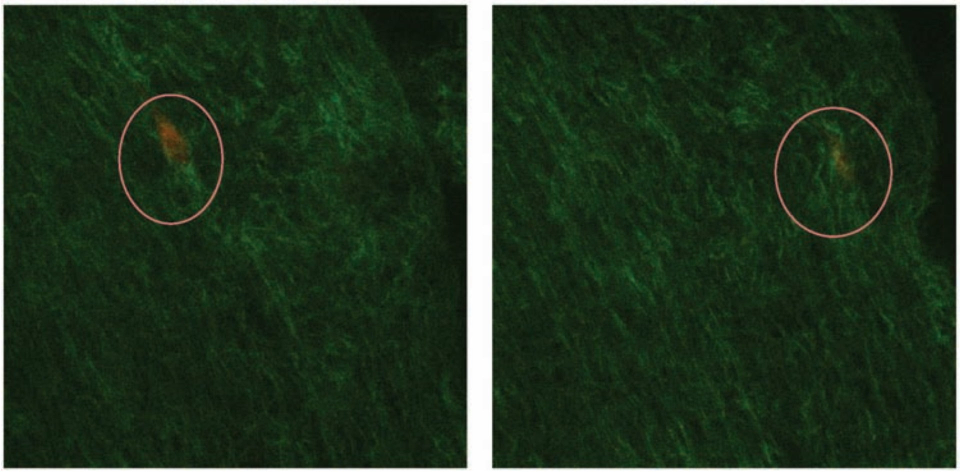

FIGURE 5. Two SHG images taken 90 µm apart within an SPH hybrid scaffold. The collagen fibers show SHG signals (green) in the SPH. Cells were stained with cell tracker (red) and a portion of it can be seen embedded in the collagen network (circled).

contrasts sharply with the lack of SHG signaling of collagen in the SIPN.

IV. B. Pre-seeded Cell Adhesion

In pre-seeded scaffolds, the collagen encourages cell spreading in the 3-D scaffold and demonstrates formation of microfilament stress fibers (Fig. 6). In the scaffolds without incorporating collagen, cells were found clumped, round in morphology, and incapable of attaching to the scaffold. Because PEGDA is not expected to promote cell adhesion, a lack of ECM cell-binding sites in non-collagenous scaffolds is presumed to be responsible for the round morphology. After 48 h, scaffolds without collagen were completely acellular. Having nothing to attach to, cells tended to migrate out of the scaffold and attach to the tissue culture plate below (not shown). Collagen-loaded scaffolds showed cell retention within the scaffold and few if any cells attached to the plate below. Collagen greatly enhanced cell spreading and retention in a 3-D manner. Stress fibers were also apparent in collagenous scaffolds, indicating that there was communication between the ECM and the cytoskeleton. Stress fibers emerged in all directions, consistent with 3-D cell adhesion.[31]

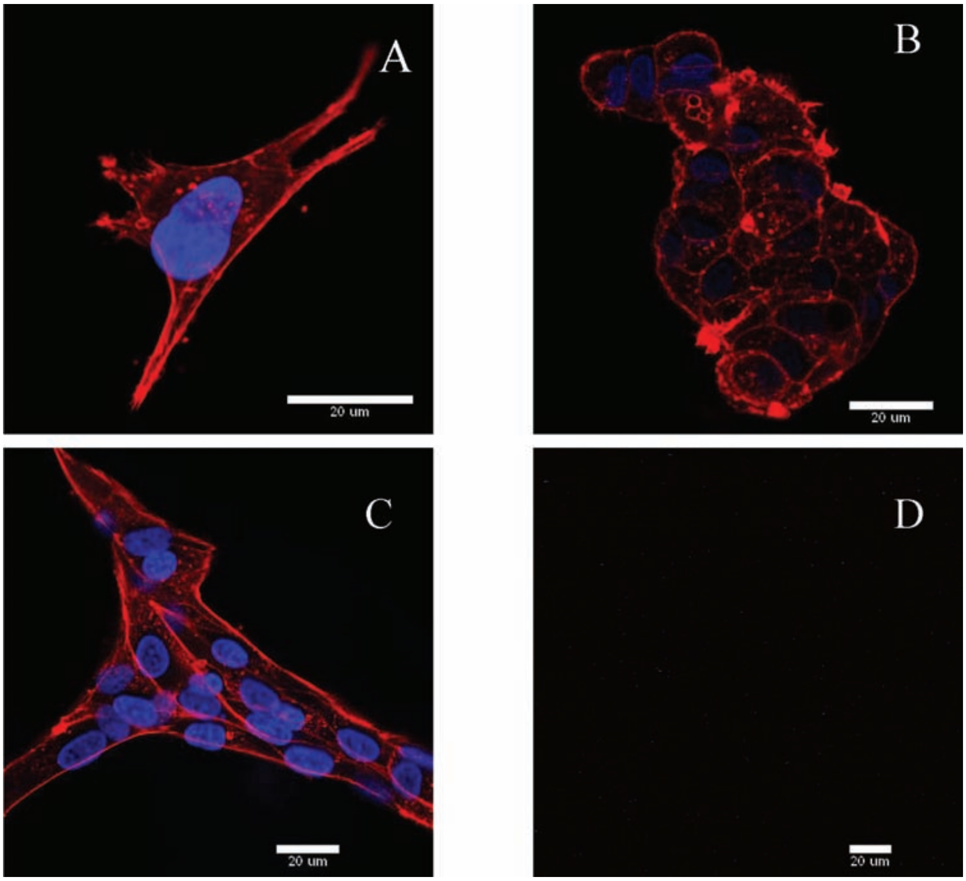

FIGURE 6. Fibroblasts have been pre-seeded in SPHs with and without collagen. After 1 d, cells in collagen already showed a spread out morphology in 3-D (A). However, cells loaded in scaffolds without collagen after 1 d did not attach, remained round, and clumped together (B). Cells in collagen gel continued to maintain the spread morphology after 2 d (C). By d 2, all cells in SPHs without collagen had migrated out (D). All cells are stained with TRITC-phalloidin (red) and DAPI (blue).

IV.C. Host Cell Integration

If cell seeding pre-implantation is not desired, we have demonstrated that this hybrid scaffold also enhanced nearby cell migration into the scaffold by virtue of an open pore structure and collagen binding. Acellular SPH scaffolds with and without collagen were placed on top of a monolayer of fibroblasts (Fig. 1). Within 3 weeks, we noticed tremendous cellular in-growth into the scaffold with collagen (Fig. 7). In

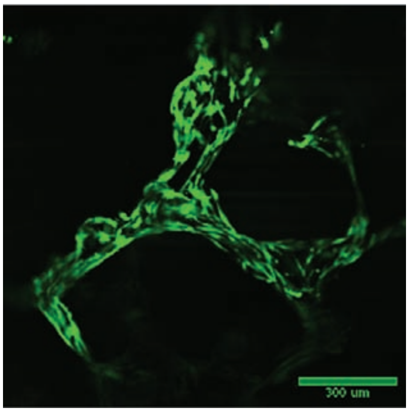

FIGURE 7. A monolayer of human fibroblasts (HT-1080 cells) were seeded on tissue culture plastic overnight. Acellular SPH scaffolds with and without collagen were placed on top of the monolayer. A live/dead assay at 3 weeks shows live cells that have migrated through the scaffold and adhered within the porous network. In SPHs without collagen, absolutely no cell in-growth was observed at any depth (not shown).

fact, in-growth was detected as early as within 3 d. The scaffold without collagen remained acellular. This demonstrates that pores alone are not sufficient for cellular in-growth, and the incorporation of collagen greatly enhances this scaffold as an ideal tissue-engineering scaffold. Good cell in-growth is necessary for in vivo implantation so that host cells can migrate into the scaffold and form a strong integration with the surrounding tissue. This is also a conduit for nerve and blood vessel in-growth that may be necessary for long-term survival of the implant (V.A.K. et al., unpublished data, 2009).

IV.D. Pore Architecture

Figure 8 shows SEM images of pore structure in three SPHs created with 100, 200, and 300 mg of sodium bicarbonate. Two types of pores

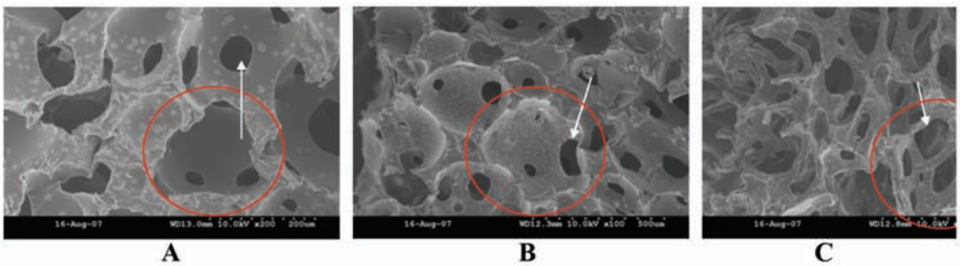

FIGURE 8. SEM images of SPHs made with 100 (A), 200 (B), and 300 (C) mg of sodium bicarbonate. Red circles indicate large pores. White arrows indicate interconnecting pores. Large pores appear similar, and the interconnecting pores seem to increase in number as sodium bicarbonate is increased. Scale bar = 500 μm.

are noticeable: larger pores are circled in red and appear similar in size and shape in each of the SPHs; smaller pores, the interconnection pathways, are indicated by white arrows. Increasing the amount of sodium bicarbonate resulted in an increased number of interconnection pores. While many investigators claim that a small pore size within a narrow range is essential to 3-D cell behavior within scaffolds,[26] our SPH hybrid technology eliminates the need for precise control of pore size or shape with respect to 3-D cell adhesion. Moreover, our method is unique in that noncovalent binding and a lack of intimate contact between scaffold materials separates the cellular microenvironment from the supporting SPH. When cells are in contact with PEGDA, despite the presence of collagen, cells are not able to spread out. Therefore, it appears that spatial and temporal separation of the two materials is necessary for optimal cell behavior.

As evident in SEM images of the pore structure, shape and size were non-uniform. However, cell morphology and adhesion in the SPH-collagen gel show similarity to purely 3-D collagen images. For that reason, SPH pore structure is not a factor contributing to cell behavior because cells do not contact the SPH. Cells in the hybrid are only embedded in the collagenous portion. Because the pores are interconnected to provide uniform distribution and effective nutrient and waste diffusion, this system does not require the stringent requirements of other systems to create a natural 3-D cell microenvironment. This system is therefore more convenient and better mimics natural living systems that generally lack the uniformity imposed by engineered constructs.

IV.E. Swelling Ratio

The differences in pore architecture caused differences in swelling ratios (Fig. 9). Swelling ratios, Q, were determined for SPHs of varying pore sizes. There was a general trend for $Q_{\text{Total water}}$ to increase as more sodium bicarbonate was used. However, $Q_{\text{Hydrogel water}}$ had no appreciable difference with different pore sizes. This indicated that differing amounts of sodium bicarbonate altered pore structure, but the amount of hydrogel in each SPH remained the same. (This phenomenon is important to note for applications in which it may be desirable to load molecules within the hydrogel structure itself). In addition, $Q_{\text{Total water}}$ was approximately 100, indicating that the SPH is capable of incorporating about 100 times its dried weight. Therefore, any long-term increases in weight due to cell proliferation or ECM production should not be barriers to long-term stability (V.A.K. et al., unpublished data, 2009).

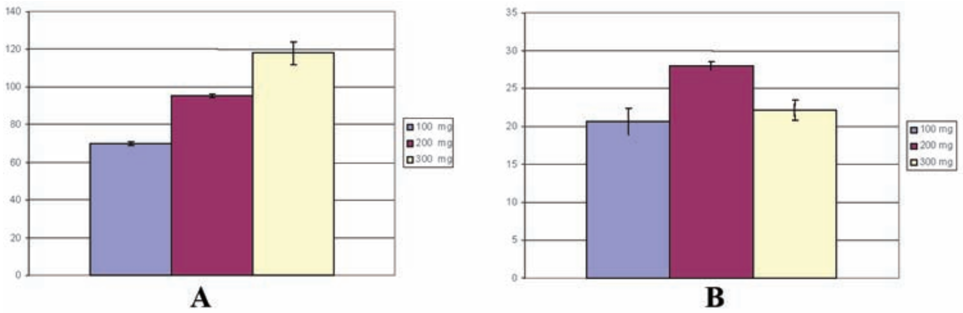

FIGURE 9. SPHs made of different amounts of sodium bicarbonate (100, 200, and 300 mg) were soaked in water. Swelling ratio of $Q_{\text{Total water}}$ (A) and $Q_{\text{Hydrogel water}}$ (B) in fold-increase (i.e., y-axis) are shown as a function of varying amount of sodium bicarbonate. When comparing their wet masses with their dry masses, the SPH made with more sodium bicarbonate had a greater swelling ratio (A). However, there was no clear trend when measuring just the swelling ratio of the hydrogel without water in the pores (B).

IV.F. Mechanical Properties

As anticipated, the contribution of collagen to the overall mechanical properties was minimal. Compressive tests showed that there was no significant difference in compressive moduli between SPHs of varying pore sizes with or without collagen. We first compared compressive moduli between 100, 200, and 300 SPHs and found no significant difference. We therefore chose the SPH created with 200 mg of sodium bicarbonate and compared compressive moduli with and without collagen. Again we noticed no significant difference. As hypothesized, the addition of collagen in the SPH did not have a significant impact on the bulk modulus. Therefore, this is a good method for maintaining a high compressive modulus overall without subjecting embedded cells to these conditions because they are only exposed to the much softer collagen microenvironment (V.A.K. et al., unpublished data, 2009). In addition, we measured the Young's modulus of the individual components as 3 kPa and 300 Pa of a 10% PEGDA gel and 1mg/mL collagen gel, respectively (Fig. 10). AFM data of hybrid structures resulted in a range of values between 300 Pa and 3kPa as the softest and strongest regions of the scaffold, respectively. The values in between are a result of testing in a nonperpendicular region of a pore.

IV.G. Optical Data

A 5% PEGDA hydrogel yielded excellent optical properties for use as a central optic. The central optic should be clear and have an appropriate

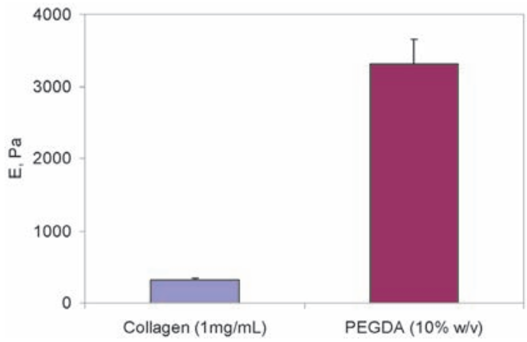

FIGURE 10. The elastic modulus as measured by AFM of collagen and PEGDA was 0.3 and 3.3 kPa, respectively. A 10% PEGDA gel is therefore about 10 times mechanically stronger than collagen gel.

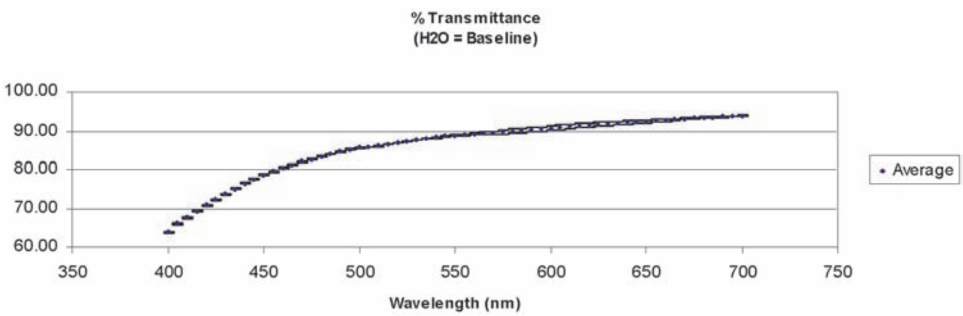

FIGURE 11. Excellent light transmission can be observed over a range of wavelengths. At 550 nm, there is about 90% transmission. As wavelength decreases, light transmission decreases, but still remains high (between 60% and 70%), likely due to the photo initiator used creating SPH. This could be promising as an implant that blocks UV light rays from penetrating through. Studies using different initiators and lower wavelengths are under investigation.

refractive index. UV-Vis spectrophotometry revealed high light transmittance over a broad range of wavelengths. For example, the average transparency at 550 nm was 90% (Fig. 11). In addition, the refractive index was approximately 1.34 (~5 brix), which is only slightly less than that of the natural cornea (1.37).

IV.H. Animal Studies

The prototype cornea implant, shown in Figure 12, consists of a core secured with the surrounding skirt by interdigitating with the superporous network. This is much different than the current cornea implants

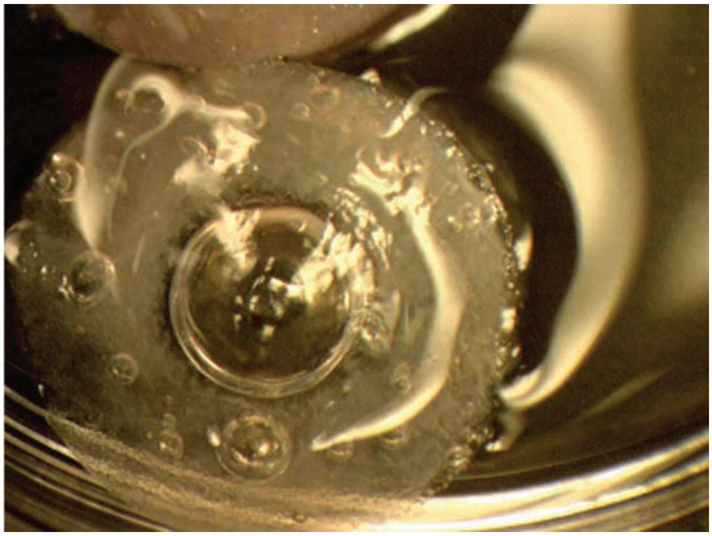

FIGURE 12. Image of the SPH cornea implant showing both core and skirt. The skirt appears white in color when collagens are incorporated in the pores. The clear ring shown between the core and skirt is indicative of successful interdigitation between the two components and, unlike other existing cornea implants, does not require a physical device to hold the core and skirt together.

such as KPro or AlphaCor. The central clear portion (i.e., the core) is clear and allows virtually unhindered light transmission, while the skirt portion is biologically active due to either the polymerized collagen network and/or pre-seeded cells. The interface between the core and skirt is visible and demonstrated successful interdigitation. The implants were well tolerated for at least 2 weeks. There was minimal inflammation and blood vessel growth. This level of inflammation is desirable in that it can help cement the scaffold within the stroma. Upon gross inspection, it appears that the hybrid scaffolds had integrated well with the surrounding tissue (Fig. 13). The degree of host cell migration between the control and hybrid groups remains to be investigated. Overall, the scaffolds were well tolerated and biocompatible, resulting in a minimal foreign body response.

V. CONCLUSION

There is often a conflict between choosing a material that can provide both natural 3-D cell bioactivity (e.g., adhesion) and the necessary mechanical strength required for a corneal prosthesis. In the current study, a unique hybrid scaffold of both synthetic and natural materials

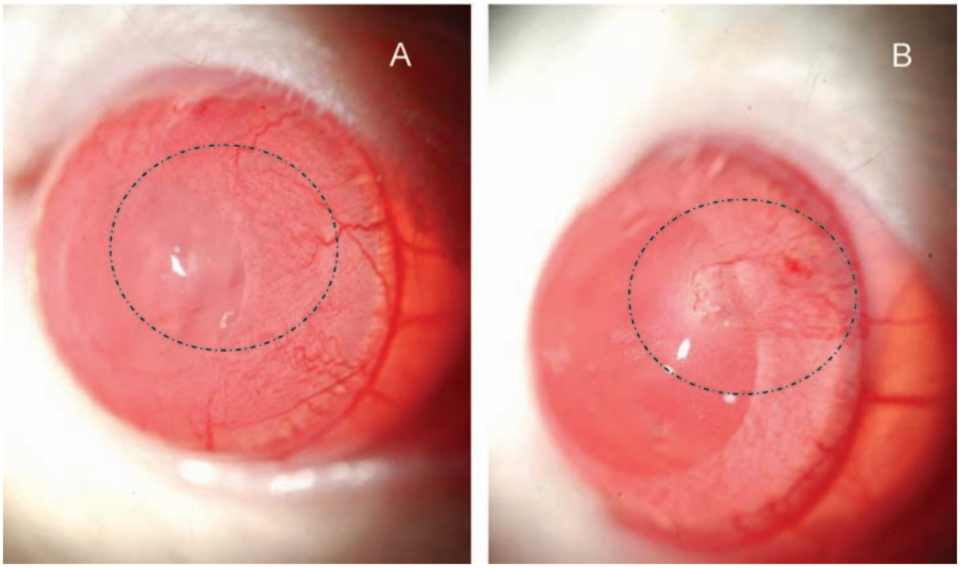

FIGURE 13. Two weeks post-implantation of SPH scaffolds by creating a small intrastromal pocket in the periphery of a rat cornea with (A) and without (B) collagen.

proved to resolve this conflict. Various biological, mechanical, and optical methods were used to determine the effects of the hybrid scaffold on cell behavior. By utilizing superporous technology and biological materials, we successfully engineered an artificial cornea that enhanced 3-D host tissue integration while maintaining adequate mechanical strength. This method proved to allow more natural cell adhesion compared, for example, with an SIPN. Further, this scaffold was engineered as an application for corneal tissue engineering. This hybrid scaffold aimed to improve upon current keratoprosthetic designs, which often lack long-term host integrations.

This new tissue-engineering method is promising in that it is a novel scaffolding method that takes advantage of both materials' advantageous properties without altering one or more materials. This method of creating a hybrid scaffold is simple, inexpensive, and versatile. By employing different materials or cell types, it can easily be extended and modified for many other tissue-engineering applications beyond the cornea.

ACKNOWLEDGMENTS

The authors thank additional individuals for contributing to the success of this study. Dr. Samantha Traphagen contributed significantly to the design for compressive testing and helped with the cell staining protocol, and Ms. Vibhooti Dev created SPH scaffolds of varying porosities. Ms. Dev and Ms. Hulda Heraldsdottir helped determine swelling ratios. Dr. Shan Sun and Dr. Joel Wise were helpful in determining an ideal collagen concentration and formulation. Dr. Gokul Kumar, Abed Namavari, and Maryam Shafiq contributed significantly to rat surgery, histology staining, and animal maintenance. We also acknowledge our funding sources: a National Institutes of Health grant (EB006067; MC), a grant from the Office of Navy Research (N00014–06–1-0100; MC), a UIC-Deiss Award (AK), and a grant from the Eye Bank Association of America (AK).

REFERENCES

1. Carlsson DJ, Li F, Shimmura S, Griffith M. Bioengineered corneas: how close are we? Curr Opin Ophthalmol. 2003;14(4):192–7.
2. "Frequently Asked Questions," Eye Bank Association of America website. Available at: http://www.restoresight.org/general/faqs.htm.
3. Eye Bank Association of America. Annual Statistical Report 2000. Washington (DC): Eye Bank Association of America; 2000.
4. Council on Scientific Affairs. Report on the organ transplant panel: Corneal Transplantation. JAMA. 1988;259:719.
5. The Collaborative Corneal Transplantation Research Group. Effectiveness of histocompatibility matching in high-risk corneal transplantation. Arch Ophthalmol. 1992;110:1392.
6. Foulks GN, Sanfilippo F. Beneficial effects of histocompatibility in high-risk corneal transplantation. Am J Ophthalmol. 1982;94(5):622–9.
7. Mader TH, Stulting RD. The high-risk penetrating keratoplasty. Ophthalmol Clin North Am. 1991;4:411.
8. Ing JJ, Ing HH, Nelson LR, Hodge DO, Bourne WM. Ten-year postoperative results of penetrating keratoplasty. Ophthalmology. 1998;105(10):1855–65.
9. Zierhut M, Pleyer U, Thiel HJ, eds. Immunology of corneal transplantation. Newton, MA: Butterworth-Heinenman, 1994.
10. Krachmer JH, Mannis MJ, Holland EJ. Cornea: fundamentals of cornea and external disease. St. Louis, MO: Mosby, 1997.
11. Caldwell DR. The soft keratoprosthesis. Trans Am Ophthalmol Soc. 1997;95:751–802.
12. Kaufman HE, Barron BA, McDonald MB. The cornea. 2nd ed. Newton, MA: Butterworth-Heinemann, 1998.
13. Artificial corneas. Wilmer Eye Institute, 2007. Available online at: http://www.hopkinsmedicine.org/wilmer/conditions/artificial_cornea.html.

14. Chirila TV. An overview of the development of artificial corneas with porous skirts and the use of PHEMA for such an application. Biomaterials. 2001;22(24):3311–7.
15. Chirila TV, Crawford GJ. A controversial episode in the history of artificial cornea: the first use of poly(methyl methacrylate). Gesnerus. 1996;53(3–4):236–42.
16. Zerbe BL, Belin MW, Ciolino JB; Boston Type 1 Keratoprosthesis Study Group. Results from the multicenter Boston Type 1 Keratoprosthesis Study. Ophthalmology. 2006 Oct;113(10):1779.
17. Johnson CS, Mian SI, Moroi S, Epstein D, Izatt J, Afshari NA. Role of corneal elasticity in damping of intraocular pressure. Invest Ophthalmol Vis Sci. 2007;48(6):2540–4.
18. Khan BF, Harissi-Dagher M, Khan DM, Dohlman CH. Advances in Boston keratoprosthesis: enhancing retention and prevention of infection and inflammation. Int Ophthalmol Clin. 2007;47(2):61–71.
19. Hicks CR, Werner L, Vijayasekaran S, Mamalis N, Apple DJ. Histology of AlphaCor skirts: evaluation of biointegration. Cornea. 2005;24(8):933–40.
20. Hicks CR, Crawford GJ, Dart JK, Grabner G, Holland EJ, Stulting RD, et al. AlphaCor: Clinical outcomes. Cornea. 2006;25(9):1034–42.
21. Coassin M, Zhang C, Green WR, Aquavella JV, Akpek EK. Histopathologic and immunologic aspects of alphacor artificial corneal failure. Am J Ophthalmol. 2007;144(5):699–704.
22. Myung D, Koh W, Bakri A, Zhang F, Marshall A, Ko J, Noolandi J, Carrasco M, Cochran JR, Frank CW, Ta CN. Design and fabrication of an artificial cornea based on a photolithographically patterned hydrogel construct. Biomed Microdevices. 2007 Dec;9(6):911–22.
23. Liu Y, Gan L, Carlsson DJ, Fagerholm P, Lagali N, Watsky MA, Munger R, Hodge WG, Priest D, Griffith M. A simple, cross- linked collagen tissue substitute for corneal implantation. Invest Ophthalmol Vis Sci. 2006 May;47(5):1869–75.
24. Duan X, Sheardown H. Dendrimer crosslinked collagen as a corneal tissue engineering scaffold: mechanical properties and corneal epithelial cell interactions. Biomaterials. 2006;27(26):4608–17.
25. Fenglan X, Yubao L, Xiaoming Y, Hongbing L, Li Z. Preparation and in vivo investigation of artificial cornea made of nano-hydroxyapatite/ poly (vinyl alcohol) hydrogel composite. J Mater Sci Mater Med. 2007;18(4):635–40.
26. Garty S, Shirakawa R, Warsen A, Ratner BD, Shen TT. Polymeric material system development for an artificial cornea to treat global blindness. Invest Ophthalmol Vis Sci. 2008;49:E-3923. Available at www.iovs.org.
27. Alaminos M, Del Carmen Sanchez-Quevedo M, Munoz-Avila JI, Serrano D, Medialdea S, Carreras I, et al. Construction of a complete rabbit

cornea substitute using a fibrin- agarose scaffold. Invest Ophthalmol Vis Sci. 2006;47(8):3311–7.

28. Stepp MA. Corneal integrins and their functions. Exp Eye Res. 2006;83(1):3–15.
29. Karande TS, Ong JL, Agrawal CM. Diffusion in musculoskeletal tissue engineering scaffolds: design issues related to porosity, permeability, architecture, and nutrient mixing. Ann Biomed Eng. 2004;32(12):1728–43.
30. Tsang VL, Bhatia SN. Three-dimensional tissue fabrication. Adv Drug Deliv Rev. 2004; 56(11):1635–47.
31. Ratner B, Hoffman A, Schoen F, Lemons J. Biomaterials science: an introduction to materials in medicine. St. Louis, MO: Academic Press, 1996.
32. Drury JL, Mooney DJ. Hydrogels for tissue engineering: scaffold design variables and applications. Biomaterials. 2003;24(24):4337–51.
33. Nguyen KT, West JL. Photopolymerizable hydrogels for tissue engineering applications. Biomaterials. 2002;23(22):4307–14.
34. Peppas NA, Barr-Howell BD. Characterization of the cross-linked structure of hydrogels. In: Peppas NA, ed. Hydrogels in medicine and pharmacy. Boca Raton, FL: CRC Press, 1987.
35. Peppas NA, Huang Y, Torres-Lugo M, Ward JH, Zhang J. Physicochemical foundations and structural design of hydrogels in medicine and biology. Annu Rev Biomed Eng. 2000;2:9–29.
36. Peppas NA, Keys KB, Torres-Lugo M, Lowman AM. Poly(ethylene glycol)-containing hydrogels in drug delivery. J Control Release 1999;62 (1–2):81–7.
37. Hill-West JL, Hubbell JA. Photopolymerized hydrogel materials for drug delivery applications. React Polym. 1995;25(1):139–47.
38. Ratner BD, Hoffman AS, Andrade JD. Synthetic hydrogels for biomedical applications. In: Hydrogels for medical and related applications. Washington, DC: American Chemical Society, 1976.
39. Andreopoulos FM, Roberts MJ, Bentley MD, Harris JM, Beckman EJ, Russell AJ. Photoimmobilization of organophosphorus hydrolase within a PEG- based hydrogel. Biotechnol Bioeng. 1999;65(5):579–88.
40. Caliceti P, Veronese FM. Improvement of the physicochemical and biopharmaceutical properties of insulin by poly(ethylene glycol) conjugation. STP Pharma Sci. 1999;9(1):107–13.
41. Halperin A, Tirrell M, Lodge TP. Tethered chains in polymer microstructures. Adv Polym Sci. 1992:10031–71.
42. Smetana K Jr. Cell biology of hydrogels. Biomaterials. 1993;14(14): 1046–1050.
43. Gemeinhart RA, Bare CM, Haasch RT, Gemeinhart EJ. Osteoblast-like cell attachment to and calcification of novel phosphonate-containing polymeric substrates. J Biomed Mater Res A. 2006;78(3):433–40.

44. Tan J, Gemeinhart RA, Ma M, Saltzman WM. Improved cell adhesion and proliferation on synthetic phosphonic acid-containing hydrogels. Biomaterials. 2005;26(17):3663- 71.
45. Fournier E, Passirani C, Montero-Menei CN, Benoit JP. Biocompatibility of implantable synthetic polymeric drug carriers: focus on brain biocompatibility. Biomaterials. 2003;24(19):3311–31.
46. Keskar V, Marion NW, Mao JJ, Gemeinhart RA. In vitro evaluation of macroporous hydrogels to facilitate stem cell infiltration, growth and differentiation. Tissue Eng Part A. 2009;15(7):1695–707.
47. Sun S, Wise J, Cho M. Human fibroblast migration in three-dimensional collagen gel in response to noninvasive electrical stimulus. I. Characterization of induced three- dimensional cell movement. Tissue Eng. 2004;10(9–10):1548–57.
48. Leonardi M, Leuenberger P, Bertrand D, Bertsch A, Renaud P. First steps toward noninvasive intraocular pressure monitoring with a sensing contact lens. Invest Ophthalmol Vis Sci. 2004;45(9):3113–7.
49. Titushkin I, Cho M. Modulation of cellular mechanics during osteogenic differentiation of human mesenchymal stem cells. Biophys J. 2007;93:3693–702.